

Blood Group B Galactosyltransferase: Insights into Substrate Binding from NMR Experiments

Jesus Angulo,[†] Brigitte Langpap,[†] Astrid Blume,[†] Thorsten Biet,[†] Bernd Meyer,[‡] N. Rama Krishna,[§] Hannelore Peters,[†] Monica M. Palcic,[⊥] and Thomas Peters^{*†}

Contribution from the Institute of Chemistry, University of Luebeck, Ratzeburger Allee 160, 23538 Luebeck, Germany, Institute of Organic Chemistry, University of Hamburg, Martin-Luther-King-Platz 6, 20146 Hamburg, Germany, University of Alabama, Birmingham, Alabama 35294-2041, and Carlsberg Laboratory, Gamle Carlsberg Vej10, DK-2500 Valby, Denmark

Received May 31, 2006; E-mail: thomas.peters@chemie.uni-luebeck.de

Abstract: The biosynthesis of human blood group B antigens is accomplished by a highly specific galactosyltransferase (GTB). On the basis of NMR experiments, we propose a “molecular tweezers mechanism” that accounts for the exquisite stereoselectivity of donor substrate selection. Transferred NOE experiments for the first time reveal the bioactive conformation of the donor substrate UDP-galactose (UDP-Gal) and of its enzymatically inactive analogue, UDP-glucose (UDP-Glc). Both bind to GTB in a folded conformation that is sparsely populated in solution, whereas acceptor ligands bind in a conformation that predominates in solution. The bound conformations of UDP-Gal and UDP-Glc are identical within experimental error. Therefore, GTB must discriminate between the two activated sugars on the basis of a hitherto unknown transition state that can only be formed in the case of UDP-Gal. A full relaxation and exchange matrix analysis of STD NMR experiments reveals that acceptor substrates dissociate significantly faster ($k_{\text{off}} > 100$ Hz) from the binding pocket than donor substrates ($k_{\text{off}} \approx 10$ Hz). STD NMR experiments also directly show that proper recognition of the hexopyranose rings of the UDP sugars requires bivalent metal cations. At the same time, this analysis furnishes the complete three-dimensional structure of the enzyme with its bound donor substrate UDP-Gal on the basis of a prior crystal structure analysis. We propose that, upon acceptor binding, GTB uses the Asp 302 and Glu 303 side chains as “molecular tweezers” to promote bound UDP-Gal but not UDP-Glc into a transition state that leads to product formation.

Introduction

The exquisite specificity with which glycosyltransferases process their substrates is still inadequately understood even though a number of high-resolution crystal structures of glycosyltransferases have been obtained in the past decade.^{1–4} The recent elucidation of the crystal structures of the human blood group A and B glycosyltransferases, an *N*-acetylgalactosaminyltransferase (GTA) and a galactosyltransferase (GTB), respectively, has been an important step toward the understanding of the catalytic mechanism of these enzymes.⁵ This study and follow-up work^{6–8} have revealed important details about

the recognition of donor and acceptor substrates. For instance, the molecular principles of discrimination between the donor substrates UDP-*N*-acetylgalactosamine (UDP-GalNAc) and UDP-galactose (UDP-Gal) became transparent and are now understood in terms of a steric effect of an amino acid substitution in the active site (i.e., a substitution of Leu 266 in GTA by a Met 266 in GTB). Only the side chain of Leu 266 allows the *N*-acetyl group of UDP-GalNAc to be accommodated in the active site.⁵ Yet other aspects of the enzyme’s specificities as well as the precise catalytic mechanism remain vague. For example, any attempts to cocrystallize UDP-Gal or UDP-GalNAc with the respective enzyme, GTB or GTA, have failed thus far, and no experimental information is available on the bound conformation of UDP-Gal or UDP-GalNAc. Also, the C-terminal loop and an internal loop that jointly close the donor binding pocket are not resolved in the crystal structures. For a closely related bovine α -1,3-galactosyltransferase, similar attempts have been made to obtain crystal structure data of UDP-Gal bound to the enzyme. Although these studies revealed interesting aspects on the binding of UDP-Gal, no data were obtained for the complex with UDP-Gal.⁹ A prior crystal-

[†] University of Luebeck.

[‡] University of Hamburg.

[§] University of Alabama.

[⊥] Carlsberg Laboratory.

- (1) Unligil, U. M.; Rini, J. M. *Curr. Opin. Struct. Biol.* **2000**, *10*, 510–517.
- (2) Breton, C.; Mucha, J.; Jeanneau, C. *Biochimie* **2001**, *83*, 713–718.
- (3) Coutinho, P. M.; Deleury, E.; Davies, G. J.; Henrissat, B. *J. Mol. Biol.* **2003**, *328*, 307–317.
- (4) Davies, G. J. *Nat. Struct. Biol.* **2001**, *8*, 98–100.
- (5) Patenaude, S. I.; Seto, N. O.; Borisova, S. N.; Szpacenko, A.; Marcus, S. L.; Palcic, M. M.; Evans, S. V. *Nat. Struct. Biol.* **2002**, *9*, 685–690.
- (6) Lee, H. J.; Barry, C. H.; Borisova, S. N.; Seto, N. O.; Zheng, R. B.; Blancher, A.; Evans, S. V.; Palcic, M. M. *J. Biol. Chem.* **2005**, *280*, 525–529.
- (7) Nguyen, H. P.; Seto, N. O.; Cai, Y.; Leinala, E. K.; Borisova, S. N.; Palcic, M. M.; Evans, S. V. *J. Biol. Chem.* **2003**, *278*, 49191–49195.

- (8) Marcus, S. L.; Polakowski, R.; Seto, N. O.; Leinala, E.; Borisova, S.; Blancher, A.; Roubinet, F.; Evans, S. V.; Palcic, M. M. *J. Biol. Chem.* **2003**, *278*, 12403–12405.

lographic study of the same enzyme reported a structure with UDP-Gal in the binding pocket,¹⁰ but unfortunately in that case the catalytic amino acid Glu 317 is covalently attached to a β -galactose residue, and it remains open, whether the bound conformation of UDP-Gal reflects the bioactive conformation, or whether this conformation is biased by the presence of the modified catalytic glutamic acid residue Glu 317. In addition, electron density in that region of the structure was poor.¹⁰ In the case of the retaining galactosyltransferase LgtC from *Neisseria meningitidis*, a donor analogue, UDP-2-deoxy-2-flouro-galactose, has been cocrystallized with the enzyme,¹¹ and for the inverting β -1,4-galactosyltransferase T1, UDP-Gal has been cocrystallized with the enzyme.¹² The bioactive conformations differ from each other, and it is problematic to predict the bioactive conformation of UDP-Gal bound to GTB on these grounds. Therefore, experimental data about the bioactive conformation of UDP-Gal are required to promote our understanding of the catalytic mechanism of GTB.

We have used NMR experiments to obtain the bioactive conformation of UDP-Gal and UDP-Glc bound to GTB and to finally solve the structure of the respective complexes. In addition, we have investigated the binding of an acceptor substrate, α -L-Fuc-(1 \rightarrow 2)- β -D-Gal-O-octyl (H-disaccharide), to GTB by NMR. The combination of transferred NOE experiments and STD NMR measurements was instrumental to obtain the missing structural details of the donor substrate–enzyme complex and in addition to reveal significant differences in the binding kinetics of donor versus acceptor substrate.

Results

Bound Conformations of UDP-Gal and UDP-Glc from Transferred NOEs. In general, transferred NOE experiments yield the bioactive conformation of a ligand bound to a receptor protein in cases where the exchange between free and bound states of the ligand is fast on the NMR relaxation time scale. In cases where low molecular weight ligands bind to large receptor proteins, transferred NOEs are easily recognized by a change of sign of the NOE. Transferred NOEs have been used in numerous examples to analyze bioactive conformations of ligands.^{13,14} In the case of UDP-Gal and UDP-Glc, small positive NOEs are observed at 500 MHz as expected for a charged molecule of this size. At 700 MHz no NOEs are observed because zero crossing conditions apply at this combination of field strength and tumbling rate of the molecule. This is an ideal condition to determine a bioactive conformation from transferred NOEs since no NOEs originating from the free state of the ligand “contaminate” the bound state information. However, first attempts to obtain transferred NOEs at 500 or at 700 MHz were not successful. Assuming a fast dissociation rate of the activated sugars, we had initially used ligand-to-protein ratios ranging from ca. 10:1 to 30:1. At 700 MHz, no NOEs were observed, and at 500 MHz the NOESY spectra obtained in the presence

of GTB were essentially identical to the ones obtained for free UDP-Gal or UDP-Glc. On the other hand, we obtained STD NMR spectra¹⁵ for UDP-Gal and for UDP-Glc indicating that ligand exchange between free and bound forms is fast enough on the relaxation time scale to generate efficient saturation transfer. A quantitative analysis of STD NMR buildup curves (see below) revealed that this is true, indeed. The dissociation rate constants k_{off} derived from these curves were ca. 10 Hz, which is uncritical for the observation of STD effects¹⁶ but which is at the limits for the observation of transferred NOEs.^{13,14} Relaxation rate matrix calculations predict that in such cases the observation of transferred NOEs becomes possible if the ligand-to-protein ratio is significantly reduced. Therefore, we repeated our experiments at a ligand-to-protein ratio of 2:1. Under these conditions, transferred NOEs become well observable as predicted from theory for a slow dissociation process.

To eliminate spin diffusion via protein protons, we used perdeuterated GTB for the transferred NOE experiments. From MALDI-TOF spectra, we estimated the extent of deuteration to be larger than 95% (data not shown). The NOESY spectra obtained for UDP-Gal and UDP-Glc in the presence of perdeuterated GTB at 700 MHz are shown in Figure 1 and unambiguously show negative NOE cross-peaks.

In both cases, we observed transferred NOEs across the diphosphate bridge that are absent in NOESY spectra of free UDP-Gal or UDP-Glc at 500 MHz (at 700 MHz no NOEs can be observed, neither for free UDP-Gal nor for UDP-Glc since zero crossing conditions apply at this field strength; see above). Therefore, the bound conformation must be dramatically different from the free conformation in solution, or, since the ligands investigated have considerable conformational flexibility,¹⁷ one should rather say that the bound conformation is not significantly populated in aqueous solution. In Figure 2, the observed transferred NOEs across the diphosphate bridge are shown schematically. The transferred NOEs between the hexopyranose rings and the ribose moieties directly show that the bound conformations of UDP-Gal and UDP-Glc are “folded-back” conformations that are not observed in solution.¹⁷

Bound Conformation of the H-Antigen Disaccharide. In contrast to the donor ligands, it was straightforward to observe transferred NOEs for acceptor ligands using “normal” ligand-to-protein ratios ranging between ca. 10:1 and 30:1. In the presence of perdeuterated GTB and in the absence of any sugar nucleotides, or UDP, negative (i.e., transferred) NOEs were observed for α -L-Fuc-(1 \rightarrow 2)- β -D-Gal-O-octyl (H-disaccharide). This in itself indicates that the dissociation rates of the acceptor ligand GTB complexes are significantly larger than those for the donor ligand GTB complexes. NOESY spectra for the H-antigen disaccharide free in solution, as well as corresponding NOESY spectra in the presence of perdeuterated GTB, are shown in Figure 3. For the free ligand key-interglycosidic NOEs across the (1 \rightarrow 2)-linkages were identified as shown in Figure 3. These NOEs are in excellent agreement with previously calculated energy maps for the α -L-Fuc-(1 \rightarrow 2)- β -D-Gal linkage.¹⁸

(9) Boix, E.; Zhang, Y.; Swaminathan, G. J.; Brew, K.; Acharya, K. R. *J. Biol. Chem.* **2002**, *277*, 28310–28318.

(10) Gastinel, L. N.; Bignon, C.; Misra, A. K.; Hindsgaul, O.; Shaper, J. H.; Joziassse, D. H. *EMBO J.* **2001**, *20*, 638–649.

(11) Persson, K.; Ly, H. D.; Dieckelmann, M.; Wakarchuk, W. W.; Withers, S. G.; Strynadka, N. C. *Nat. Struct. Biol.* **2001**, *8*, 166–175.

(12) Ramakrishnan, B.; Balaji, P. V.; Qasba, P. K. *J. Mol. Biol.* **2002**, *318*, 491–502.

(13) Neuhaus, D.; Williamson, M. P. *The Nuclear Overhauser Effect in Structural and Conformational Analysis*; Wiley-VCH: New York, 2000.

(14) Ni, F. *Prog. Nucl. Magn. Reson. Spectrosc.* **1994**, *26*, 517–606.

(15) Mayer, M.; Meyer, B. *Angew. Chem., Int. Ed.* **1999**, *38*, 1784–1788.

(16) Jayalakshmi, V.; Krishna, N. R. *J. Magn. Reson.* **2002**, *155*, 106–118.

(17) Monteiro, C.; Hervé du Penhoat, C. Activated Sugars. In *NMR Spectroscopy of Glycoconjugates*; Jiménez-Barbero, J., Peters, T., Eds.; Wiley-VCH: Weinheim, 2003; pp 247–271.

(18) Imberty, A.; Pérez, S. *Glycobiology* **1994**, *4*, 351–366.

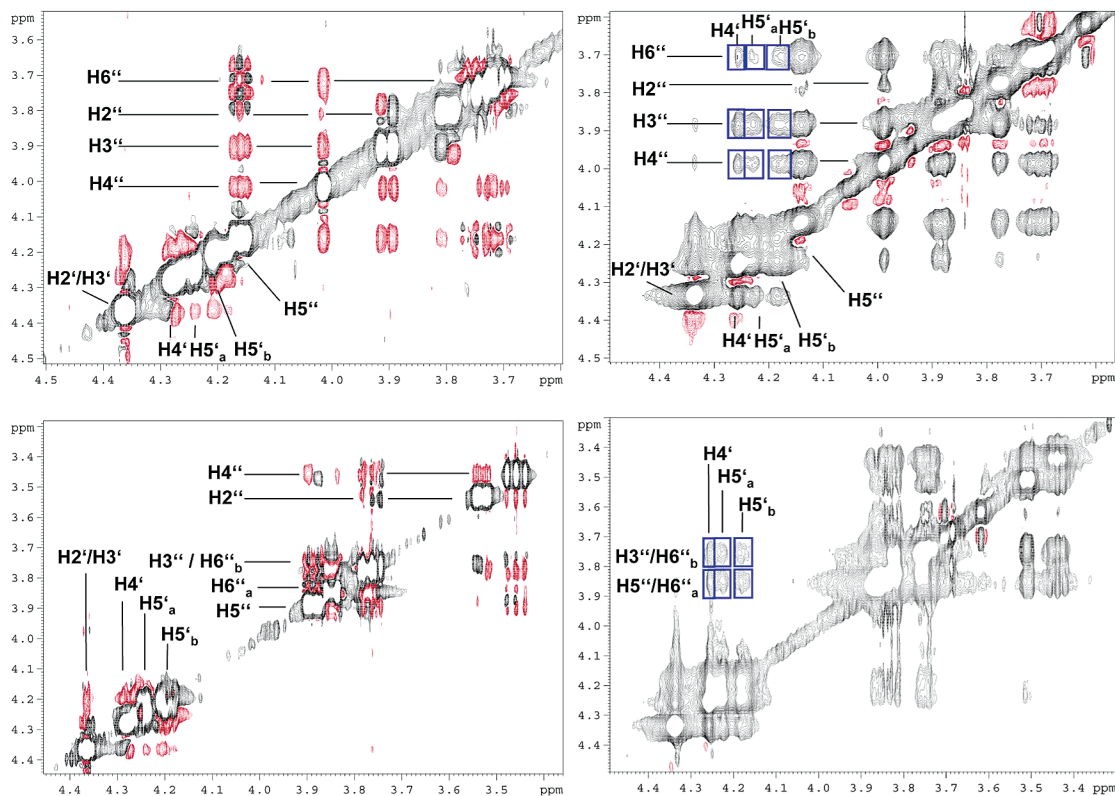


Figure 1. Conformational change of the sugar nucleotides upon binding to GTB. NOESY spectra of UDP-Gal (top) and UDP-Glc (bottom) in the presence (right panels) and in the absence (left panels) of GTB. Spectra were recorded at 700 (right panels) and 500 MHz (left panels). NOEs across the pyrophosphate bridge (blue squares) are only observed for the bound states of UDP-Gal and UDP-Glc.

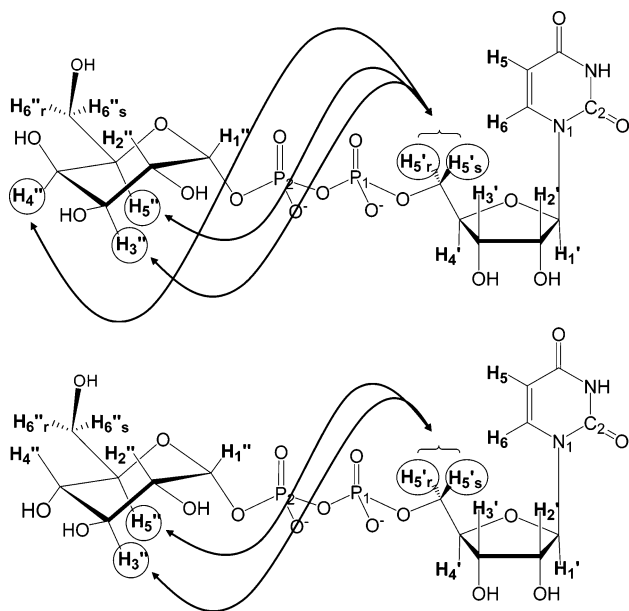


Figure 2. Key inter-residue NOEs of UDP-Gal (top) and UDP-Glc (bottom) bound to GTB. The transferred NOEs shown reflect a folded-back conformation of the ligands in the bound state.

A qualitative analysis of the transferred NOEs observed for the acceptor ligand reveals only minor conformational disturbances around the glycosidic linkage upon binding to GTB (i.e., a reduction of the relative intensity of the H1'–H2 interglycosidic NOE in comparison to the free state of the ligands; cf. Figure 3). It is concluded that the bioactive conformation of the acceptor ligand is very similar to the most populated conformation in aqueous solution.

Bivalent Metal Ions Trigger the Recognition of the Pyranose Moiety of UDP-Gal and UDP-Glc. It is well-documented that bivalent cations such as Mg^{2+} and Mn^{2+} have a significant impact on the function of glycosyltransferases.^{19–21} With NMR, we directly observed the conformational transitions that occur upon binding of the donor ligands, UDP-Gal and UDP-Glc, to GTB in the presence of Mg^{2+} . First, we recorded a series of STD NMR spectra (Figure 4) of UDP-Gal and UDP-Glc in the presence of GTB and Mg^{2+} .

STD signals were observed for the uracil and ribose moieties as well as for the pyranose unit. From these spectra, binding epitopes were derived that indicate that the activated sugars are completely buried in the binding pocket (Figure 4). Removal of Mg^{2+} by addition of perdeuterated EDTA led to dramatically altered STD spectra. It is obvious that the enzyme still binds to the activated sugars but only the base and the ribose moiety are receiving notable amounts of saturation. No STD effects were observed for the pyranose units (Figure 4). Upon addition of Mg^{2+} to this sample, we obtained the original STD spectra with a clear response from the pyranose rings. This shows that the process is reversible, and that proper “recognition” of UDP-Gal or UDP-Glc is triggered by Mg^{2+} . It should be noted that the presence of even high concentrations of Mg^{2+} in the absence of GTB does not in itself induce a conformational change toward the folded-back conformation (for corresponding NOESY spectra cf. Supporting Information). Proper “folding” of UDP-Gal requires the presence of both Mg^{2+} and GTB.

(19) Zhang, Y.; Wang, P. G.; Brew, K. *J. Biol. Chem.* **2001**, *276*, 11567–11574.

(20) Tarbouriech, N.; Chamock, S. J.; Davies, G. J. *J. Mol. Biol.* **2001**, *314*, 655–661.

(21) Petrova, P.; Koca, J.; Imberty, A. *Eur. J. Biochem.* **2001**, *268*, 5365–5374.

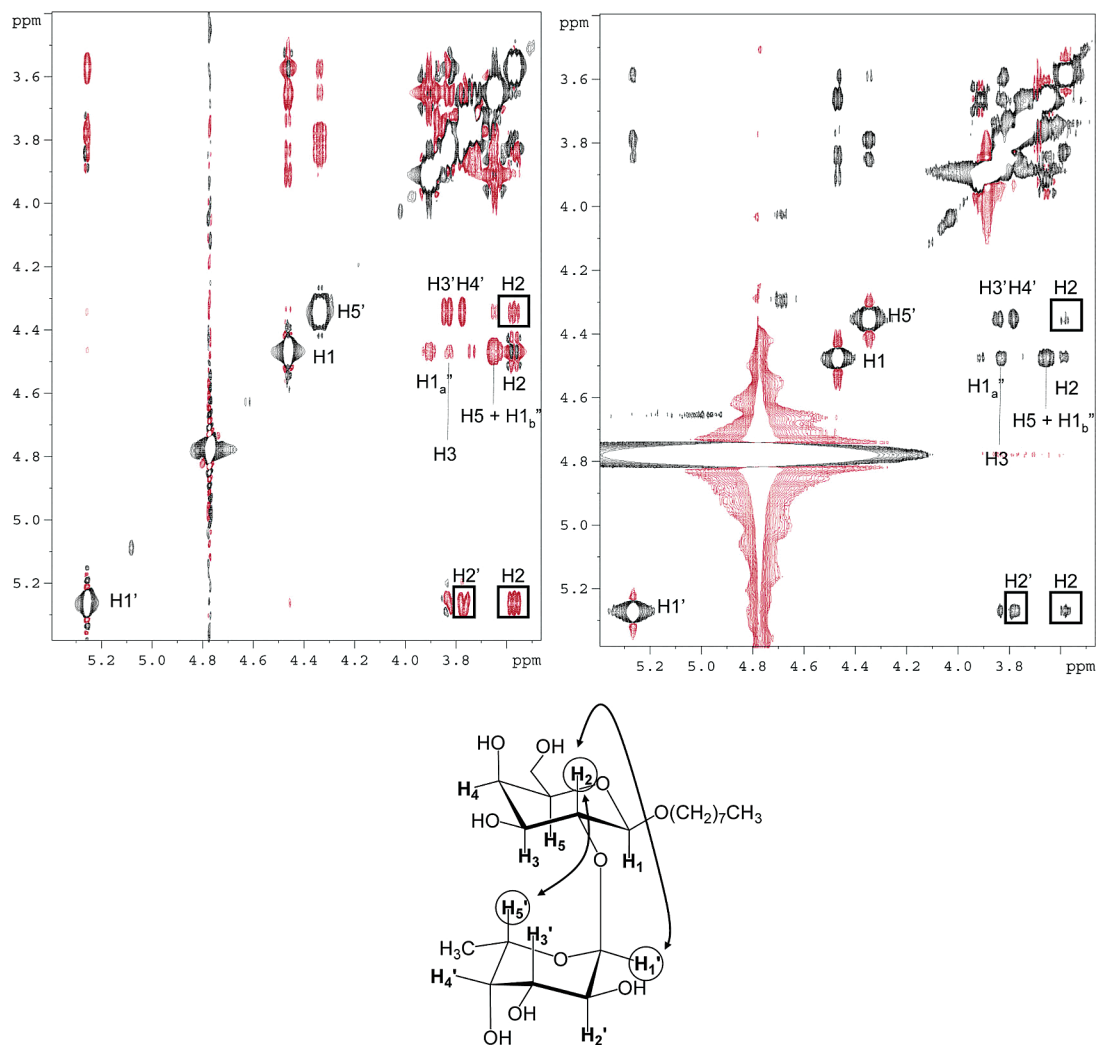


Figure 3. GTB binds to acceptor ligands in a conformation that predominates in solution. (Top) NOESY spectra of the H-disaccharide in the presence (right panel) and in the absence (left panel) of GTB. (Bottom) Schematic representation of key interglycosidic NOEs (cross-peaks enclosed by squares in the spectra). Spectra were recorded at 500 MHz and show that no significant conformational changes occur upon binding.

We then performed transferred NOE experiments in the absence and in the presence of Mg^{2+} (cf. Supporting Information) and in the presence of GTB. These experiments unambiguously show that in the absence of Mg^{2+} the folded-back bioactive conformation is no longer present, at least not in quantities that allow the observation of the corresponding transferred NOEs across the diphosphate bridge. Addition of Mg^{2+} to this sample refurbished the original transferred NOE patterns (i.e., the folded-back conformation was restored). To summarize, STD NMR experiments and transferred NOEs indicate binding of UDP-Gal and UDP-Glc even in the absence of Mg^{2+} albeit with a different, most likely extended, bound conformation.

UDP-Gal and UDP-Glc Have Identical Binding Modes.

In an accompanying study, we investigated the relative binding affinities of UDP-Gal and UDP-Glc to GTB. It turns out that the two ligands bind to GTB with practically the same affinity.²² Here, we compare the binding epitopes of UDP-Gal and UDP-Glc in detail. Usually, binding epitopes are derived from relative STD values measured for a given saturation time.²³ To compare

the binding epitopes of UDP-Gal and UDP-Glc, we acquired STD effects as a function of the saturation time, called STD buildup curves, for both ligands (Figure 5).

The advantage of this method is that a more reliable comparison can be made. It turns out that the STD buildup curves are identical within experimental error except for the protons $\text{H4}''$ and $\text{H1}''$ of the pyranose (Gal or Glc) unit. This is in excellent agreement with the accompanying study that shows that UDP-Gal and UDP-Glc have practically identical dissociation constants.²² The discrepancy for $\text{H4}''$ is expected because of the different stereochemistry at $\text{C4}''$. Even without any further analysis, the almost perfect match of the STD buildup curves shows that the binding epitopes, and therefore the overall binding modes of UDP-Gal and UDP-Glc, are identical within experimental error. To summarize, the STD buildup curves serve as “fingerprints” that reflect the bound conformation as well as the binding mode of the two sugar nucleotides.

Binding Kinetics of Donor and Acceptor Ligands from an STD-Based Model of the UDP-Gal/GTB Complex. A subsequent quantitative analysis of STD buildup curves for UDP-Gal and UDP-Glc binding to GTB directly reveals the binding kinetics. We analyzed the buildup curves utilizing two

(22) Blume, A.; Angulo, J.; Biet, T.; Peters, H.; Benie, A. J.; Palcic, M. M.; Peters, T. *J. Biol. Chem.* **2006**, in press.

(23) Mayer, M.; Meyer, B. *J. Am. Chem. Soc.* **2001**, *123*, 6108–6117.

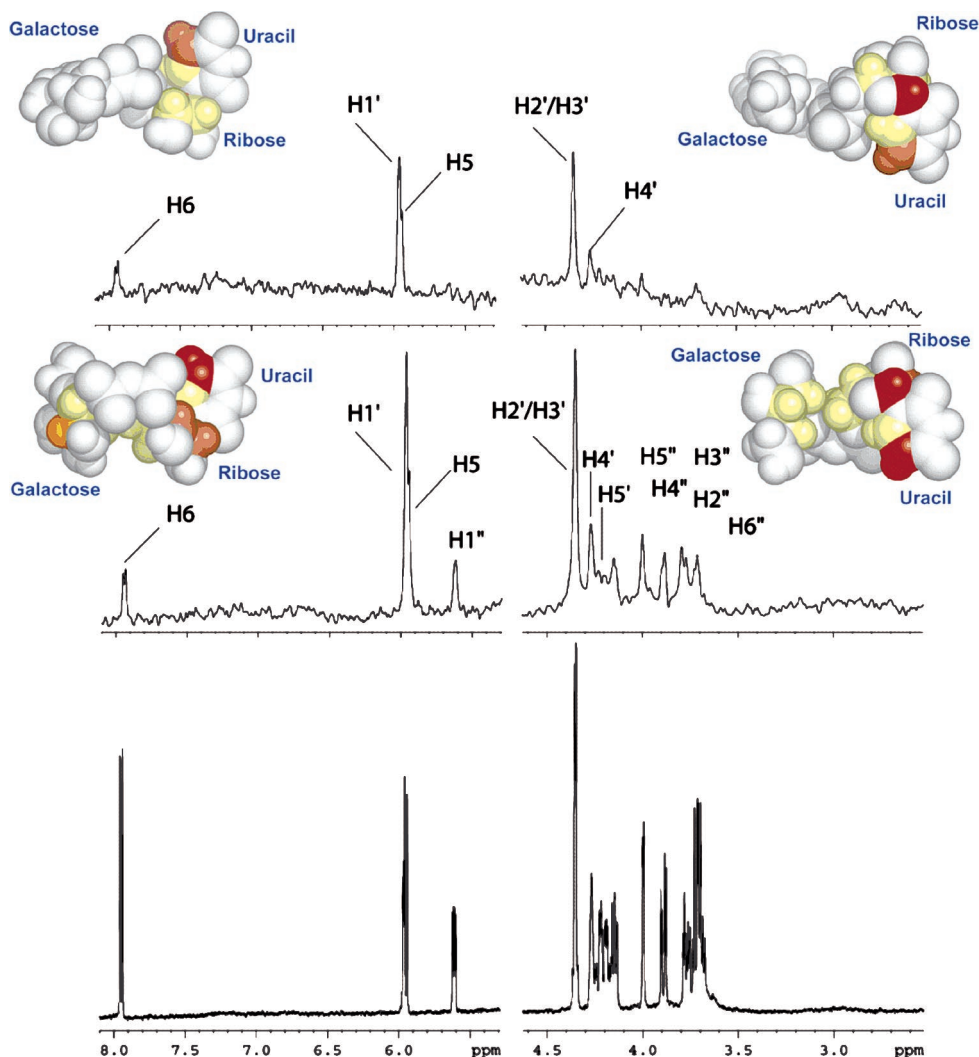


Figure 4. Mg^{2+} ions trigger the proper recognition of the hexopyranose ring of UDP-Gal. STD NMR spectra of UDP-Gal in the presence of GTB and in the absence (top) or presence (middle) of Mg^{2+} . (Bottom) Reference spectrum of UDP-Gal. It is obvious that protons of the galactose ring give an STD response only if Mg^{2+} is present indicating that only in this case the pyranose unit is properly “recognized” by the enzyme. The corresponding spectra for UDP-Glc are very similar and are shown in the Supporting Information. The models shown as inserts reflect the binding epitope as determined from relative STD values (color code: red 80–100%, brown 60–80%, orange 40–60%, pale yellow 20–40%, white 0–20%). The models also reflect the bound conformation with and without Mg^{2+} .

approaches. First, we applied the program CORCEMA-ST¹⁶ to calculate theoretical STD effects based on the full relaxation and exchange rate matrix. For the calculations, we assumed a K_D value of 17 μM for both UDP-Gal and UDP-Glc as estimated from the K_{ib} value for UDP-Gal.²⁴ The crystal structure of GTB⁵ (pdb entry: 1lzj) provided a starting point to generate a structure of the UDP-Gal/GTB complex based on our experimental NOE and STD restraints. Full relaxation and exchange rate matrix calculations require consideration of the contribution of all protein protons within a given radius around the ligand. Two loops that were disordered and not resolved in the crystal structure were expected to generate contacts with the ligands. We modeled these loops into the crystal structure using the program COMPOSER as part of the SYBYL program suite. The crystal structure of bovine $\alpha 3GalT^{10}$ (pdb entry: 1k4v) was used as a template for the homology modeling of the loops. Residues from Trp181 to Cys196, as well as those from His348 to Arg352, were considered as belonging to structurally

conserved regions (helices $\alpha 4$ and $\alpha 7$ in $\alpha 3GalT$, respectively). The remaining parts were modeled using a database of more than 5000 loops using the BIOPOLYMER module of SYBYL. After attaching a galactose or a glucose residue to the UDP moiety already present in the crystal structure, we subjected the resulting model to docking calculations with AutoDock 3.0. Interestingly, the best solutions from these docking experiments were in excellent agreement with the distance restraints (cf. Figure 2) obtained from transferred NOE experiments that had established folded-back bound conformations of UDP-Gal and UDP-Glc yielding an experimentally validated model of GTB with UDP-Gal or UDP-Glc bound to GTB (Figure 6).

Then, STD buildup curves were analyzed by applying complete relaxation and exchange rate matrix calculations with the program CORCEMA-ST using the bound conformations of the donor ligand obtained from the docking calculations. On the basis of the structures obtained for the UDP-Gal/GTB and the UDP-Glc/GTB complex, we calculated STD buildup curves as a function of the off rate. A comparison with corresponding experimental STD buildup curves then delivered the off rates

(24) Seto, N. O.; Compston, C. A.; Evans, S. V.; Bundle, D. R.; Narang, S. A.; Palcic, M. M. *Eur. J. Biochem.* **1999**, *259*, 770–775.

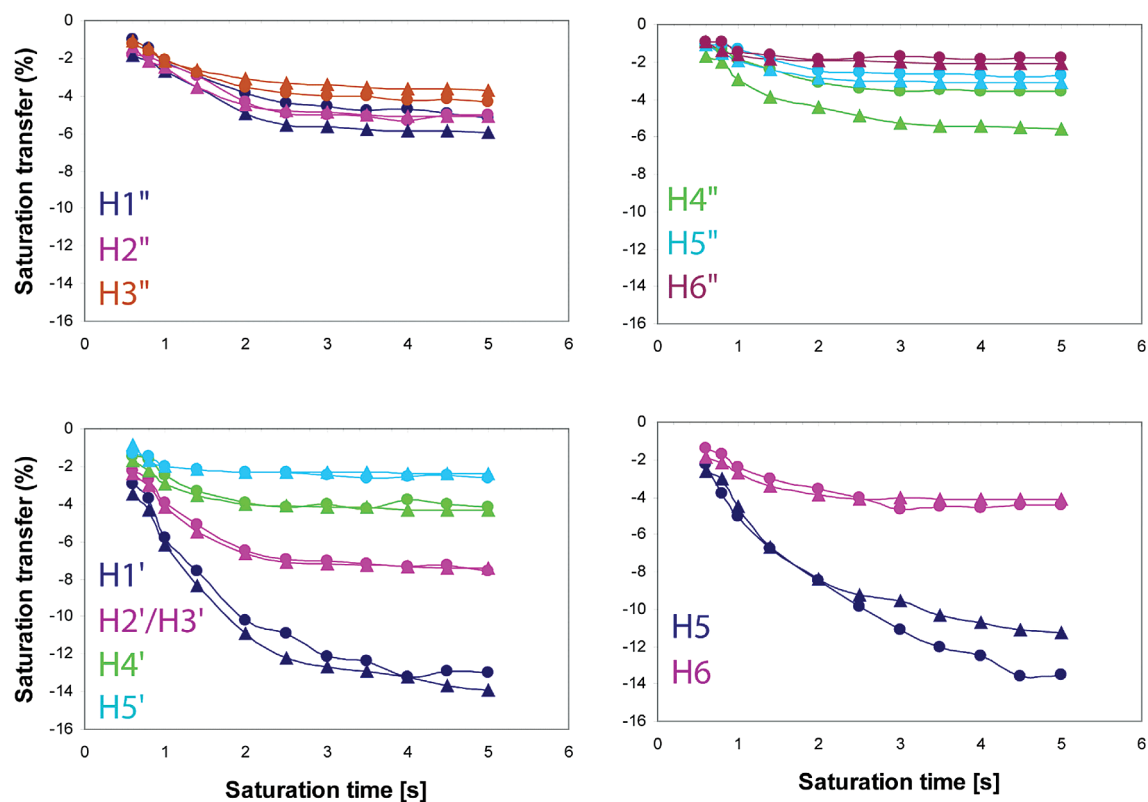


Figure 5. STD buildup curves provide a “fingerprint” for the bound conformations of UDP-Gal and UDP-Glc. STD buildup curves measured at 500 MHz for UDP-Gal (●) and UDP-Glc (▲) bound to GTB are overlaid. The level of saturation of ligand protons is shown as a function of the saturation time (hexopyranose rings: top panels; ribose rings: bottom, left panel; uracil rings: bottom, right panel).

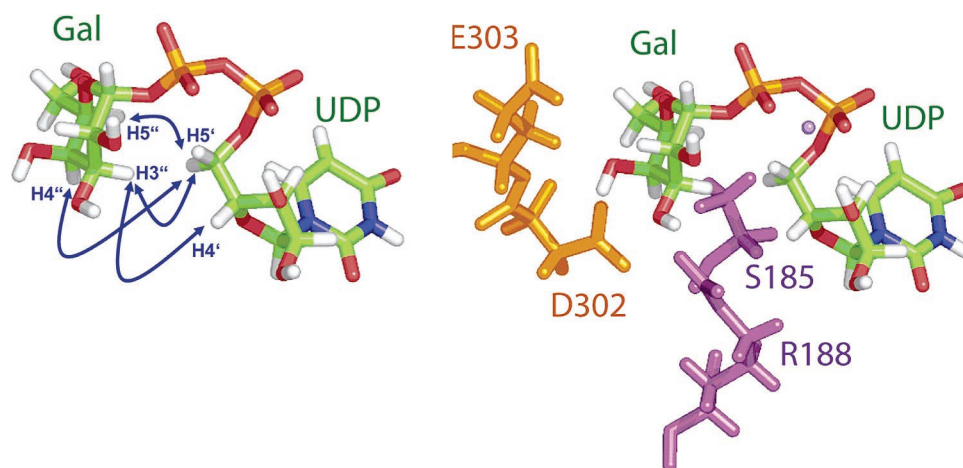


Figure 6. Model of GTB and folded-back conformation of bound UDP-Gal (coordinates are available upon request from the authors). (Left) Conformation of UDP-Gal that gives the best R -NOE factor (0.19) with the STD data and that is in agreement with the transferred NOEs across the diphosphate bridge (blue arrows). (Right) UDP-Gal in the binding pocket of GTB. Residues E303 and D302 (orange) are also present in the X-ray structure.⁵ Residues S185 and R188 (magenta) belong to disordered loops that have been modeled by homology for the present study. The purple ball symbolizes the position of the Mg^{2+} that is held in place by a DXD motif.⁵

with which donor and acceptor substrates dissociate from their respective binding pockets. The minimum R value¹⁶ as a function of k_{off} then identifies the “true” off rate. The result of this analysis is illustrated in Figure 7, which depicts the largest relative STD effects of the donor ($H1'$ of ribose) and of the acceptor ($H4'$ of galactose).

For UDP-Gal, this led to an excellent fit between experimental and calculated STD buildup curves for an off rate constant k_{off} of 10 Hz (Figure 7) yielding a corresponding on rate constant k_{on} of $5.9 \times 10^5 \text{ M}^{-1} \text{ s}^{-1}$. This relatively low off rate positions the complex in a range where the observation of transferred

NOEs becomes critical since the exchange process between free and bound forms of the ligand becomes slow on the relaxation time scale. This is in excellent agreement with the results of the transferred NOE experiments reported above, which qualitatively indicates a relatively slow dissociation process. In contrast to this, STD buildup curves for the acceptor ligand reveal a much faster dissociation rate utilizing the same protocol as described above. Assuming a K_D value of $40 \mu\text{M}$ as determined from surface plasmon resonance experiments, we determined the dissociation rate k_{off} to be above at least 100 Hz (Figure 7), which is a factor of 10 larger than that observed

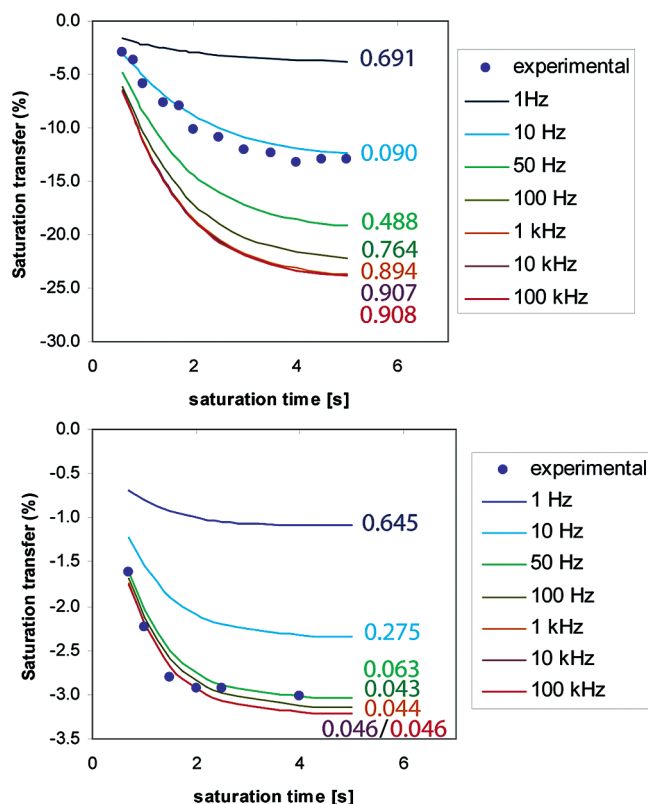


Figure 7. Different kinetics of the binding of donors and acceptor ligands to the enzyme GTB. The figure shows the experimental buildup curves (dots) for the most intense STD signals of UDP-Gal (H1' of ribose; top) and the H-antigen (H4' of the galactose; bottom), as well as the STD curves predicted from full relaxation rate matrix calculations with the model of the complex, using different values of the dissociation rate (k_{off}). R -factors for each proton as a function of k_{off} are color-coded. For UDP-Gal, an excellent match is obtained for $k_{\text{off}} = 10$ Hz. For the H-antigen, the best fits are obtained for a range of k_{off} values between 100 and up to 100 000 Hz.

for UDP-Gal or UDP-Glc. The precise off rate was not determined in this case since the STD effects were relatively insensitive to varying off rates over a wide range up to 10 kHz. This is expected according to theoretical considerations that predict STD effects to become independent of K_{D} values when two conditions are simultaneously satisfied, viz., the exchange is fast on the relaxation rate scale and one is using high ligand/protein ratios.¹⁶ From this, the lower limit for the on rate constant k_{on} is calculated as $2.5 \times 10^7 \text{ M}^{-1} \text{ s}^{-1}$.

As mentioned earlier, the full relaxation and exchange matrix analysis of the STD curves at the same time delivers an experimental verification of our docking model (Figure 6) of the complex of UDP-Gal and UDP-Glc with GTB. This model is the starting point for further structural refinements using CORCEMA-ST that are currently underway in our laboratory.

Discussion

This NMR study delivers new structural and mechanistic details for the human blood group B galactosyltransferase binding to its donor and acceptor substrates. As one major result, we identified the conformation of UDP-Gal bound to GTB (cf. Figure 6) utilizing transferred NOEs. Interestingly, this folded-back bioactive conformation is not significantly populated in aqueous solution. Only binding to the enzyme stabilizes this conformational state. A comparison with crystal structure data

is possible for the case of another retaining galactosyltransferase LgtC from *N. meningitidis* where a crystal structure (pdb entry: pdb 1g9r) has been obtained for the complex of the enzyme with a donor substrate analogue, UDP-2-fluoro-galactose.¹¹ A comparison of UDP-Gal bound to GTB with UDP-2-fluoro-galactose complexed to LgtC reveals that the two bioactive conformations are similar, with differences in the relative orientation of the galactose to the ribose moiety. Since we have used perdeuterated GTB to acquire transfer NOESY spectra, we have minimized spin diffusion via protein protons, and it is valid to qualitatively correlate the size of transferred NOEs with corresponding proton-proton distances. The proton-proton distances across the diphosphate bridge found for UDP-Gal bound to LgtC would predict, for example, that the relative size of the NOE between any of the protons attached to C5' of ribose and H4'' would be the largest NOE across the diphosphate bridge, and in fact about as large as the intraglycosidic NOE between H3'' of galactose and H5'' of galactose. A quick inspection of the NOESY spectrum of UDP-Gal bound to GTB in Figure 1 unambiguously shows that this is not the case. This suggests that transfer NOE experiments are ideally suited to analyze the bioactive conformations of UDP-Gal bound to different galactosyltransferases, and NOE buildup curves will provide more quantitative data in the future.

An inspection of the bioactive conformation of UDP-Gal bound to GTB suggests that it may be possible to introduce a tether between C6'' of galactose and C5 of uracil that would lock the bioactive conformation. Such a compound may represent a useful tool for cocrystallization experiments. According to previous studies,²⁵ the OH group attached to C6'' of galactose is of minor importance as deoxygenation of this position leads to a donor substrate that is still active. Therefore, tethering of C6'' with C5 should be feasible. The same study²⁵ also reports the activities of all other deoxygenated UDP-Gal derivatives. It is interesting to note that the 4-deoxy derivative is almost inactive, supporting our conclusions about the important role of the OH-4'' group of UDP-Gal.

The analysis of the bioactive conformation of the H-disaccharide, an acceptor substrate, revealed fewer surprises. The acceptor binds to GTB in a conformation that is predominant in aqueous solution. This is in accordance with previous crystal structure data.^{5,7}

A quantitative evaluation of the UDP-Gal/GTB complex has been based on STD NMR data. With the program CORCEMA-ST, we have validated the bioactive conformations of UDP-Gal bound to GTB. The overall R factor of 0.19 (cf. Materials and Methods) implies that the model presented here is already of high quality and thus substantiates the bioactive conformation of UDP-Gal bound to GTB. In the case of the acceptor substrate, the quantitative analysis leads to less satisfying R factors, indicating that our model still needs refinement. Nevertheless, the gross conformational features are in accordance with prior crystal structure analysis data.

More interestingly, the quantitative analysis of the STD NMR data for the first time reveals data on the kinetics of donor and acceptor substrates binding to GTB. On the basis of NMR experiments, we suggest a mechanistic model (Figures 6 and 8) for the GTB-catalyzed transfer of galactose from UDP-Gal

(25) Sujino, K.; Uchiyama, T.; Hindsgaul, O.; Seto, N. O. L.; Wakarchuk, W. W.; Palcic, M. M. *J. Am. Chem. Soc.* **2000**, *122*, 1261–1269.

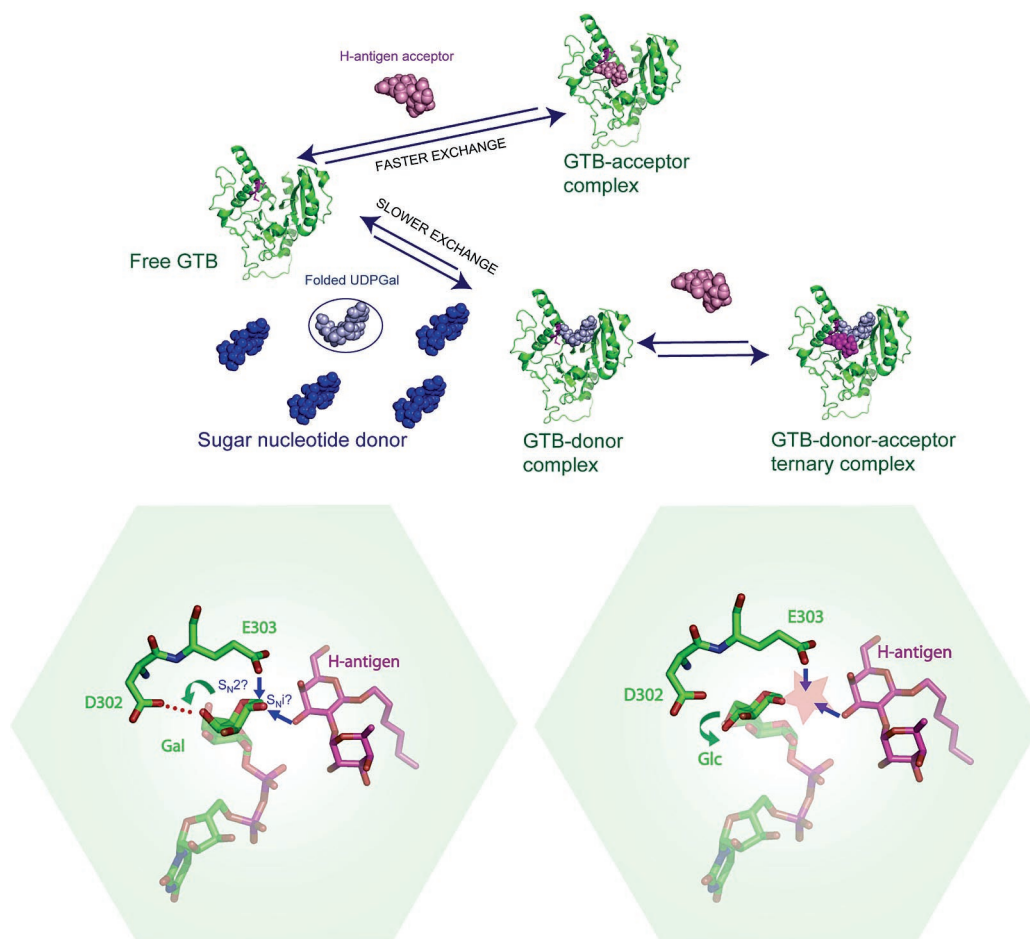


Figure 8. Tweezers mechanism. Two key amino acids in the binding pocket, D302 and E303, interact with the galactose residue of UDP-Gal (bottom left) to position it correctly for the transfer to the H-antigen. UDP-Glc (bottom right) exposes OH-4' in the "wrong direction" and cannot be promoted to a transition state. From the different off rates for the donor and acceptor substrates, it is concluded that first UDP-Gal is bound to the enzyme (top). The subsequent binding of an acceptor substrate induces an unknown conformational transition that leads to the transfer of the galactose residue.

onto an H-type acceptor substrate. This model helps to explain why the enzyme selectively processes UDP-Gal and not UDP-Glc, although the bioactive conformations as well as the binding epitopes of the two sugars are almost identical.

In the first step, GTB binds to a conformer of UDP-Gal that is sparsely populated in aqueous solution. For this step, the presence of a bivalent metal cation such as Mg^{2+} is essential to assist conformer selection and to stabilize the folded-back bioactive conformation of the substrate to finally allow proper recognition of the galactose residue. This complex is characterized by a relatively long residence time of the ligand of ca. 100 ms. In the second step, the acceptor substrate binds to GTB to form a ternary complex and to induce the transfer of the galactose moiety from UDP-Gal to the acceptor. The binding of the acceptor substrate is characterized by a much shorter lifetime of the ternary complex of at most 10 ms. Our data cannot discriminate between the possibilities of a double inversion S_N2 -type mechanism and a concerted S_Ni mechanism.

Upon binding of the acceptor, only UDP-Gal but not UDP-Glc undergoes a further conformational transition that presumably leads to the transition state required for the galactose transfer. The model reveals that Asp 302 and Glu 303 act like tweezers that lock the galactose unit "in place" while the conformational transition toward the transition state occurs (Figure 8). To achieve this lock, Asp 302 forms a hydrogen

bond with OH-4' and Glu 303 interacts with the anomeric carbon in the sense of an S_N2 attack.

For UDP-Glc, this "tweezers mechanism" is impossible as the OH-4' group is pointing in the wrong direction (Figure 8). This model also suggests that the bioactive conformation that we observe in transferred NOE experiments is not a transition state but an intermediate that still requires presumably acceptor ligand-induced conformational changes for the transfer reaction to occur.

The enzyme thus has developed a mechanism to protect the donor substrate for the subsequent transfer reaction by slowing down the dissociation reaction relative to the binding kinetics of the acceptor ligand. The distinct binding kinetics of the donor and the acceptor substrate suggest that the enzyme in general must first bind to the donor substrate for a successful transfer to occur. Binding of the acceptor substrate alone will most likely not be productive.

To summarize, we propose an ordered catalytic mechanism that consists of the following steps (cf. Figure 8):

(1) Recognition of a sparsely populated folded-back conformation of UDP-Gal (the lifetime of the bound conformation is in the range of 100 ms). The enzyme stabilizes UDP-Gal in its bioactive conformation and protects it against hydrolysis.

(2) Acceptor binding occurs with an *on-off* kinetics that is at least an order of magnitude faster than that for the donor

substrate (the lifetime of the bound acceptor is less than ca. 10 ms). Concomitant with the acceptor binding, a “molecular tweezers assisted” promotion of UDP-Gal into the transition state occurs.

(3) Transfer of the galactose, and fast release of the product.

A comparison with structural data available from the literature reveals that analogous structural motifs exist for other retaining galactosyltransferases (e.g., the bovine α 3GalT^{10,26} or the bacterial galactosyltransferase LgtC).¹¹ This indicates that the “tweezers mechanism” may be of general applicability.

For the proper design of specific glycosyltransferase inhibitors, it is of utmost importance to understand the precise mechanism by which these enzymes discriminate their substrates. Here, we have described subtle mechanistic details for the discrimination of two substrates that are structurally extremely similar and that cannot be derived from, for example, crystal structure data alone. In this case, NMR experiments have delivered missing information that, in conjunction with prior X-ray data, leads to a significantly improved understanding of the donor substrate specificity of GTB.

Materials and Methods

Protein Preparation and General Materials. Recombinant GTB enzyme was overexpressed in *Escherichia coli* BL21 cells following the same protocol as described previously²⁷ and purified by successive chromatography on SP Sepharose Fast Flow and UDP-hexanol amine. Uniformly ¹⁵N,²H-labeled GTB was overexpressed under aerobic conditions at 37 °C over 14 h following the labeling protocol of Marley et al.²⁸ in minimal medium with 0.1% ¹⁵NH₄Cl, 0.4% *d*₇-glucose (Cambridge Isotope), and 0.4% *d*₈-glycerol (Cambridge Isotope) in deuterated M9 salts KD₂PO₄, Na₂DPO₄ (50 mM, pH 7.2–7.5), 0.05% NaCl, 4 mM MgSO₄, 0.1 mM CaCl₂, 1 μ M FeSO₄/CoCl₂, vitamin solution BME (Sigma) diluted 1:100, 10% *E. coli* DN OD3 (Silantes), and 200 μ g/mL ampicillin in D₂O. A quantity of 120 mg/L ¹⁵N,²H-labeled GTB was purified as already described.²⁷ Disodium salts of UDP-Gal and UDP-Glc and DL-1,4-dithiothreitol-*d*₁₀ (DTT) were purchased from Sigma-Aldrich. The radioactive analogue UDP-(¹⁴C)-Gal was from Amersham Biosciences as a lithium salt. Uniformly deuterated 2,2-bis(hydroxymethyl)-2,2',2''-nitrilotriethanol (BisTris) was purchased from Cambridge Isotope Lab. The H-antigen disaccharide was available in our research group.²⁹

Preparation of the NMR Samples. After purification of the enzyme, the samples in 50 mM MOPS buffer pH 7 were exchanged to deuterated 50 mM Bistris, pH 6.8, in D₂O containing 5 mM of deuterated β -mercaptoethanol via centrifugal filtering using Amicon Ultra filter devices (Millipore). Protein concentration was measured by using a colorimetric method based on the Bradford assay performed on ELISA plates. Enzyme activities were checked by a radiochemical assay using UDP-(¹⁴C)-Gal. All NMR samples were prepared in 180 μ L of buffer solution and measured using 3-mm NMR tubes. Samples for STD NMR contained 20 μ M of GTB and 1 mM of ligand (protein/ligand ratio 1:50). For NOE experiments of the free ligands, a concentration of 5 mM was used in the same buffer as for STD and trNOE experiments. For transferred NOE experiments with the acceptor ligands the concentrations were 130 μ M perdeuterated GTB and 1.3 mM ligand at a protein/ligand ratio of 1:10. For the donor ligands UDP-Gal, UDP-Glc, and UDP-GlcNAc, 200–300 μ M of perdeuterated enzyme and 400–600 μ M of ligand were used, resulting in a protein/ligand ratio

of 1:2. For the STD NMR experiments in the absence of Mg²⁺ ions, 1 mM EDTA-*d*₁₂ was added to each sample containing only ligand and protein. For the transferred NOE without divalent cations, 10 mM EDTA-*d*₁₂ was used, as the protein concentrations were also ca. 10 times higher. To carry out the experiments with Mg²⁺ ions, 10 and 20 mM MgCl₂ were added to the same samples, respectively.

STD NMR Measurements. All STD NMR experiments were carried out on a Bruker Avance DRX 500 spectrometer equipped with a 5-mm inverse triple-resonance probe head. Spectra were performed at 288 K using the standard pulse sequence²³ with a 10-ms spin-lock pulse ($T_1\rho$ filter; field strength of 7.4 kHz) to reduce the background protein resonances and to facilitate the data analysis. In all cases, a uniformly ²H,¹⁵N-labeled protein sample was used. Presaturation of the protein NMR signals of the enzyme was performed using a train of selective Gaussian pulses of a duration of 49 ms each and separated by a short delay of 1 ms (field strength of 73 Hz, referring to a 33.33 kHz rectangular hard pulse and corresponding to a flip angle of approximately 720°). For the STD buildup curves, the number of selective pulses was varied to achieve different saturation times. The on-resonance frequencies were 0 ppm for the experiments with the sugar nucleotide ligands and 7.2 ppm for the experiments involving the acceptor ligands. Off-resonance irradiation was applied at 40 ppm where no NMR resonances are present. For the group epitope mapping analysis of the ligands, relative STD values for the protons were calculated by arbitrarily assigning a value of 100% to the most intense STD signal.

Transferred NOE Experiments. For the H-antigen, transferred NOE experiments were carried out on a Bruker Avance DRX 500 spectrometer equipped with a 5-mm inverse triple-resonance probe head. To study the sugar nucleotides, highest sensitivity was critical, and therefore in this case the experiments were performed on a Bruker Avance DRX 700 spectrometer equipped with a 5-mm triple-resonance cryoprobe. In all cases, uniformly ²H,¹⁵N-labeled protein (level of deuteration > 95%) was used. This suppresses protein-mediated spin diffusion as a contribution to trNOE cross-peaks. Spectra were recorded at 288 K for the acceptor ligands, and at a slightly lower temperature (280 K) for the donors, to reduce the hydrolysis reaction of UDP-Gal in the presence of the enzyme at such low ligand/protein ratios. The residual water signal (HDO) was removed using a Watergate W5 solvent suppression scheme. Mixing times ranged from 100 to 250 ms for the ligands in the presence of the protein and were set at 600 ms for the ligands in the absence of GTB. For the donor ligands, NOESY experiments were performed at different mixing times ranging from 200 ms to 1 s at 700 MHz and 280 K in the absence of GTB. These spectra showed no NOEs at all because zero crossing conditions apply at this field strength and the given tumbling rate of the ligand. Therefore, NOESY spectra of the donor ligands in the absence of GTB were obtained at 500 MHz at 298 K.

Quantitative Analysis of STD NMR Curves To Analyze the Binding Kinetics of Donor and Acceptor Ligands. For the homology modeling and loop predictions, we used the SYBYL program package including the COMPOSER module (Tripos Associates). Docking calculations were performed with AutoDock 3.0. STD buildup curves were analyzed by applying complete relaxation and exchange rate matrix calculations with the program CORCEMA-ST. To reduce the dimensions of the matrixes, only nonexchangeable protein protons within a distance of 8 Å to ligand protons were included. Since the protein signals were saturated at 0 ppm, and no assignment for this enzyme is currently available, we have made the assumption that only the methyl protons of Val, Leu, and Ile were saturated instantaneously, except in the cases of Ile123-H δ 2, Val175-H γ , Val210-H γ 2, Val212-H γ 1, Val344-H γ 1, Ile192-H δ 1, and Val351-H γ , since their proximity to deshielding aromatic ring currents as observed in the crystal structure of GTB should displace their chemical shifts significantly downfield compared to their expected random coil values. A K_D of 17 μ M was used for UDP-Gal and UDP-Glc, taking the K_{ib} experimentally determined for UDP-Gal as an estimate.²⁴ For the H-antigen, a K_D of

(26) Boix, E.; Swaminathan, G. J.; Zhang, Y.; Natesh, R.; Brew, K.; Acharya, K. R. *J. Biol. Chem.* **2001**, *276*, 48608–48614.

(27) Seto, N. O.; Palcic, M. M.; Hinds-gaul, O.; Bundle, D. R.; Narang, S. A. *Eur. J. Biochem.* **1995**, *234*, 323–328.

(28) Marley, J.; Lu, M.; Bracken, C. *J. Biomol. NMR* **2001**, *20*, 71–75.

(29) Kamath, V. P.; Yeske, R. E.; Gregson, J. M.; Ratcliffe, R. M.; Fang, Y. R.; Palcic, M. M. *Carbohydr. Res.* **2004**, *339*, 1141–1146.

40 μM was determined experimentally by surface plasmon resonance. During the calculations, the K_{D} values were kept constant, and k_{off} was varied from 1 to 10^4 Hz. The best fit between experimental and calculated STD values was determined using the NOE R factor.¹⁶ For UDP-Gal, an overall R factor of 0.19 for the protons H5, H6, H1', H2'/H3', H4', H5a'/H5b', H1'', H2'', H3'', H4'', H5'', and H6a''/H6b'' was obtained ($k_{\text{off}} = 10$ Hz, $K_{\text{D}} = 17$ μM). For the H-disaccharide, the overall R factor for the protons H1'', H5'', H1', H2', H3', H4', and H5' was 0.35 ($k_{\text{off}} = 100$ Hz, $K_{\text{D}} = 40$ μM).

Acknowledgment. T.P. and B.M. thank the *Deutsche Forschungsgemeinschaft* for grants within the *Sonderforschungsbereich 470* (Projects B2 and B3) and for a grant for the 700 MHz NMR (Me 1830/1). J.A. thanks the European Union for a Marie-Curie Intra-European Fellowship (MEIF-CT-2003-500861). We thank Prof. Dr. Buko Lindner from the Research Center Borstel for the acquisition of MALDI-TOF spectra. We

would especially like to thank Dr. Jayalakshmi Venkatanarayanan for assistance in implementing and using CORCEMA-ST calculations.

Supporting Information Available: (1) NOESY spectra of UDP-Gal in the presence of GTB and in the absence of Mg^{2+} ions (top) and upon addition of Mg^{2+} to the same sample (bottom); (2) NOESY spectra of UDP-Glc in the presence of GTB and in the absence of Mg^{2+} ions (top) and upon addition of Mg^{2+} to the same sample (bottom); (3) STD NMR spectra of UDP-Glc in the presence of GTB and in the absence (top) or presence (middle) of Mg^{2+} ; and (4) NOESY spectra of UDP-Gal in the absence of Mg^{2+} ions (top) and upon addition of an excess of Mg^{2+} to the same sample (bottom). This material is available free of charge via the Internet at <http://pubs.acs.org>.

JA063550R